

Non-Markovian dynamics of reaction coordinate in polymer folding

Peer-reviewed author version

Sakaue, T.; Walter, J. -C.; Carlon, E. & VANDERZANDE, Carlo (2017)

Non-Markovian dynamics of reaction coordinate in polymer folding. In: SOFT MATTER, 13(17), p. 3174-3181.

DOI: 10.1039/c7sm00395a

Handle: <http://hdl.handle.net/1942/24210>

Non-Markovian dynamics of reaction coordinate in polymer folding

T. Sakaue

*Department of Physics, Kyushu University, Fukuoka 819-0395, Japan and
JST, PRESTO, 4-1-8 Honcho Kawaguchi, Saitama 332-0012, Japan*

J.-C. Walter

*Laboratoire Charles Coulomb, UMR5221 CNRS-UM, Université de Montpellier,
Place Eugène Bataillon, 34095 Montpellier Cedex 5, France*

E. Carlon

Institute for Theoretical Physics, KU Leuven, Celestijnenlaan 200D, B-3001 Leuven, Belgium

C. Vanderzande

*Faculty of Sciences, Hasselt University, Agoralaan 1, B-3590 Diepenbeek, Belgium and
Institute for Theoretical Physics, KU Leuven, Celestijnenlaan 200D, B-3001 Leuven, Belgium
(Dated: February 20, 2017)*

We develop a theoretical description of the critical zipping dynamics of a self-folding polymer. We use tension propagation theory and the formalism of the generalized Langevin equation applied to a polymer that contains two complementary parts which can bind to each other. At the critical temperature, the (un)zipping is unbiased and the two strands opens and closes as a zipper. The number of closed base pairs $n(t)$ displays a subdiffusive motion characterized by a variance growing as $\langle \Delta n^2(t) \rangle \sim t^\alpha$ with $\alpha < 1$ at long times. Our theory provides an estimate of both the asymptotic anomalous exponent α and of the subleading correction term, which are both in excellent agreement with numerical simulations. The results indicate that the tension propagation theory captures the relevant features of the dynamics and shed some new insights on related polymer problems characterized by anomalous dynamical behavior.

I. INTRODUCTION

Conformational dynamics of biopolymers, such as DNA, RNA and proteins, is a complex process involving a large number of degrees of freedom. Like any other many-body problem, the concept of the *reaction coordinate* (RC) is often invoked in its coarse grained description. One may be tempted to assume Markovian dynamics for the RC such that the problem is amenable to standard stochastic analysis [1]. However, the validity of such a simple approach requires that the RC is the slowest variable and that its characteristic time scale is well separated from all other time scales in the problem. This condition is not easily met in many situations, giving rise to non-Markovian effects and anomalous dynamics.

Anomalous diffusion is an ubiquitous phenomenon observed in a large number of experimental systems or in computer simulations [2–11]. Characteristic of these systems is a mean squared displacement (MSD) of particle positions (or more generally of some RC) which scales asymptotically in time as $\langle \Delta \vec{x}^2(t) \rangle \sim t^\alpha$ with $\alpha \neq 1$, i.e. deviating from the Brownian motion predictions. The evidence of anomalous dynamics is mostly, both in experiments and simulations, of observational/empirical nature. Due to the complexity of the systems studied it is hard to predict the value of α from theoretical inputs.

In this paper, we investigate the anomalous diffusion of the RC in a simple system with folding dynamics: the (un)zipping in hairpin forming polymers [12]. This process is illustrated in Fig. 1. The polymer contains

two complementary parts which can bind to each other and fluctuates between an open (unzipped) and a closed (zipped) conformation. We focus here to the dynamics at the transition temperature where zipped and unzipped state have the same equilibrium free energy. The natural RC for the system is the number of broken base pairs $n(t)$, see Fig. 1. The time series of $n(t)$ exhibits back and forth fluctuations reminiscent to Brownian motion. Simulations of the mean-square displacement (MSD) reveals the motion is sub-diffusive $\langle \Delta n^2(t) \rangle \sim t^\alpha$ with $\alpha < 1$ [13].

Here, we clarify the non-Markovian nature of this process using an analysis of the collective dynamics of the polymer, based on the tension propagation along the polymer backbone. A perturbation propagates along the backbone due to the tension transmitted along the chain, generating long range temporal correlations. The theory enables us to provide an analytical estimate of α including the sub-leading term. Our predictions are in very good agreement with the results of computer simulations, which demonstrates the validity of our approach and sheds new insight on related polymer problems characterized by anomalous diffusion.

The theory is based on the Generalized Langevin Equation (GLE) formalism, which is briefly reviewed in Sec. II. The key point is the calculation of the memory kernel entering in the GLE and characterizing the non-Markovian aspects of the dynamics. This calculation is done in Sec. III and allows to estimate both the leading exponent α and the subleading term. In Sec. IV we show that the analytical predictions are in excellent agreement with nu-

merical simulations of the (un)zipping process. Finally, in Sec. V, we present our conclusions and we point out the relation of our results to the problems of tagged monomer motion and polymer translocation.

II. GENERALIZED LANGEVIN EQUATION

Consider a step displacement applied to an appropriate RC $\vec{z}(t)$. Let us monitor the subsequent average force $\vec{f}(t)$ to keep the given displacement. This protocol can be analyzed by the force balance equation

$$\int_{t_0}^t d\tau \gamma(t-\tau) \vec{v}(\tau) = \vec{f}(t) \quad (1)$$

where $\vec{v}(t) = d\vec{z}(t)/dt$ and $\gamma(t)$ is the memory kernel (in Markovian systems $\gamma(t) \sim \delta(t)$). In Eq. (1) we may set the lower bound of the time integral as $t_0 \rightarrow -\infty$ by assuming the system is already in the equilibrium state before the operation is made. In the case of a step displacement \vec{u} imposed at $t = 0$, i.e., $\vec{z}(t+0) = \vec{z}(t-0) + \vec{u}$, we have $\vec{v}(t) = \vec{u}\delta(t)$, the above equation is reduced to

$$u\gamma(t) = f(t) \quad (2)$$

where we have switched to a scalar notation by noting $\vec{u} \parallel \vec{f}$ in isotropic system.

To connect the average stress relaxation with the anomalous fluctuating dynamics, we need to look at each realization of the stochastic processes by adding the thermal noise term $\vec{\xi}(t)$ to the right-hand side of Eq. (1). The noise has zero mean $\langle \xi_i(t) \rangle = 0$, and it is related to the memory kernel via the fluctuation-dissipation theorem (FDT) $\langle \xi_i(t) \xi_i(\tau) \rangle = k_B T \gamma(|t-\tau|) \delta_{ij}$. The equivalent expression of the Generalized Langevin Equation (GLE) is

$$\vec{v}(t) = \int_{t_0}^t d\tau \mu(t-\tau) \vec{f}(\tau) + \vec{\eta}(t) \quad (3)$$

where $\mu(t)$ is the mobility kernel with the FDT $\langle \eta_i(t) \eta_j(\tau) \rangle = k_B T \mu(|t-\tau|) \delta_{ij}$. In the next section a power-law decaying memory function $\gamma(t) \sim t^{-\alpha}$ in the case of polymer pulling is derived from polymer tension propagation arguments. From this one derives $\mu(t) \sim -t^{\alpha-2}$ (for details see Appendix). In the unbiased case $\vec{f}(t) = 0$, the MSD can be derived after integration of the velocity correlation function $\langle \vec{v}(t) \cdot \vec{v}(s) \rangle = \langle \vec{\eta}(t) \cdot \vec{\eta}(s) \rangle$ twice with respect to time, yielding $\langle \Delta \vec{z}(t)^2 \rangle \sim t^\alpha$, i.e., the stress relaxation exponent characterizing the decay of the memory kernel $\gamma(t)$ is equal to the MSD exponent.

III. MEMORY KERNEL FOR ZIPPING DYNAMICS

Before dealing with the more complex case of zipping polymers, it is useful to recall some known results [14, 15]

for a simpler case of polymer pulling. Let us suppose that one end of an equilibrated polymer is displaced by Δx at $t = 0$ and that the position of that monomer is kept fixed. This operation produces a stretching of the end part of the chain. Through tension propagation the polymer relaxes to a new equilibrium state shifted with respect to the original position. The longest relaxation time is $\tau_R \simeq \tau_0 N^{z\nu}$, where τ_0 is a monomer time scale, $\nu \simeq 3/5$ is the Flory exponent and the $z = 2 + 1/\nu$ is the dynamical exponent (we consider here the free draining case, if hydrodynamic interactions are taken into account $z = 3$). At a time $t < \tau_R$ only $m(t)$ monomer close to the displaced end are stretched, while the remaining $N - m(t)$ at the opposite end do not yet feel the displacement operation. The longest relaxation time for a fragment containing m monomers is $t \simeq \tau_0 m^{\nu z}$, from which one finds

$$m(t) \simeq \left(\frac{t}{\tau_0} \right)^{\frac{1}{\nu z}} \quad (4)$$

which gives how m grows in time. To keep the end monomer at a fixed position one needs to apply a force $f(t)$ which can be estimated using polymer entropic elasticity. An equilibrated polymer stretched by Δx exerts a force at its two ends which is equal to:

$$f \simeq \frac{k_B T}{\langle R^2 \rangle} \Delta x \quad (5)$$

where $\langle R^2 \rangle$ indicates the average of the squared end-to-end distance. Applying the previous relation to the stretched $m(t)$ monomers, for which $\langle R^2 \rangle \simeq a^2 m^{2\nu}$ and using Eq. (4) we obtain

$$\gamma(t) = \frac{f(t)}{\Delta x} \simeq \frac{k_B T}{a^2} \left(\frac{t}{\tau_0} \right)^{-2/z} \quad (6)$$

where we used Eq. (2) for a step displacement equal to Δx . Equation (6) gives the memory kernel associated to the step displacement of a polymer end. According to the discussion of the previous section the decay exponent of $\gamma(t)$ is equal to the MSD exponent. Hence we obtain $\alpha = 2/z$. For an ideal Rouse chain for which $z = 4$ ($\nu = 1/2$), one obtains a tagged monomer diffusion with MSD scaling as $\Delta \vec{x}^2(t) \sim t^{1/2}$, which is in agreement with the exact solution from Rouse dynamics. More generally the tension propagation dynamics leads to a subdiffusive behavior with $\alpha = 2\nu/(1+2\nu) < 1$, which turns into ordinary diffusion at times $t > \tau_R$.

We turn now to the case of zipping dynamics. Let us assume that the polymer is in equilibrium with n_0 bonds from the tail being in unzipped state, while the remaining $N - n_0$ bonds are zipped, i.e., the monomer's label at the fork point is $n(t) = n_0$ ($t < 0$). Consider now an instantaneous break of $\Delta n (= \mathcal{O}(1))$ zipped pairs at the fork point creating Δn additional unzipped monomer pairs. This operation produces (i) the change of the reaction coordinate $n(t) = n_0 \rightarrow n_0 + \Delta n$ and (ii) the displacement of the position of the fork in real space

$\vec{r}(n_0, 0) \rightarrow \vec{r}(n_0 + \Delta n, 0)$, where $\vec{r}(n, t)$ is the position of the monomer n at time t (Fig. 1). As in the pulling problem the entire chain cannot respond to the break of Δn bonds all at once. At time t smaller than the longest relaxation time of the polymer only a finite section, i.e., $m(t)$ bonds given close to the fork point respond to the perturbation.

The deformation of such a responding part of the chain can be evaluated as (Fig. 1)

$$\begin{aligned} \Delta R_m(t) &\simeq a\Delta n + a\{m(t) - \Delta n\}^\nu - am(t)^\nu \\ &\simeq a[\Delta n - \nu\Delta n m(t)^{\nu-1}] \end{aligned} \quad (7)$$

where we have taken $m(t) \gg \Delta n$ and expanded to lowest order in Δn . The growth of $m(t)$ in time is governed by the tension propagation dynamics of Eq. (4). The force necessary to hold the fork point to the new position $n_0 + \Delta n$ can be estimated again from entropic elasticity (Eq. (5)) as

$$\begin{aligned} f(t) &\simeq \frac{k_B T}{\langle R^2(t) \rangle} \Delta R_m(t) \\ &\simeq \frac{k_B T}{a} \Delta n \left[\left(\frac{t}{\tau_0} \right)^{-2/z} - \nu \left(\frac{t}{\tau_0} \right)^{-\frac{1+\nu}{\nu z}} \right] \end{aligned} \quad (8)$$

Dividing by $a\Delta n$ we obtain the memory kernel with a leading t behavior as in Eq. (6), but now the analysis unveils the presence of a sub-leading term. The calculation of the MSD which follows from Eq. (8) is given in the Appendix, where the full calculation of $\gamma(t)$ is presented including the subleading term. The final result for the RC dynamics is

$$\langle \Delta n^2(t) \rangle \sim t^{2/(\nu z)} \left(1 + C t^{-(1-\nu)/(\nu z)} \right) \quad (9)$$

with C a positive constant.

IV. NUMERICAL RESULTS

The model used in the simulations is discussed in details in Ref. [13] and was also employed in previous studies of renaturation dynamics [16]. We consider two strands with L monomers which are joined to a common monomer, labeled with $i = 0$, while we use an index $i = 1 \dots L$ to label the monomers on the two strands. Only monomers with the same index i on the two strands can bind with binding energy ε . The dynamics consists of lattice corner-flips or end-flips local moves which are randomly generated by a Monte Carlo algorithm. This algorithm was shown to reproduce the Rouse model dynamics in previous studies [17] and represents an interesting and efficient alternative to the more commonly used Langevin dynamics for polymers in the continuum.

A Monte Carlo move not respecting mutual or self-avoidance between the two strands is rejected. A move binding two monomers on the opposite strands is always accepted, while the opposite move of unbinding

is accepted with a probability $\exp(-\beta\varepsilon) < 1$, where $\beta = 1/k_B T$ is the inverse temperature. The algorithm hence satisfies detailed balance. The temperature is tuned to the critical value $\beta = \beta_c$, which is very accurately known as it relies on previous high precision data about polymers on an fcc lattices [18]. In addition in the model bubbles are not allowed to form so the dynamics is strictly sequential as in a zipper.

A simulation run is initialized by setting the fork point to $n(t = 0) = L/2$, so that monomers $0 \leq i \leq L/2$ are bound and $i > L/2$ are unbound. The initial configuration is equilibrated by sufficiently long Monte Carlo runs while keeping the fork point fixed. After equilibration, the constraint is released and the actual simulation is started. The fork point performs a stochastic back and forth motion along the polymer backbone until one of the two ends is reached and the simulation is stopped. We monitor in particular the MSD $\langle \Delta n^2(t) \rangle$ and the average duration time of the process τ .

The analysis of Ref. [13] showed that the dynamics is well-described by a fractional brownian motion (fBm) characterized by a Hurst exponent $H = 0.44(1)$ (recall that in fBm the Hurst exponent is linked to the MSD exponent by the relation $\alpha = 2H = 0.88(2)$ and that the fBm is described by a GLE). The analytical prediction of Eq. (9) is $\alpha = 2/(\nu z) = 0.92$, which is somewhat higher than the numerical value of Ref. [13]. Figure 2(a) shows a plot of the MSD for lattice polymers of lengths up to $N = 768$ and averaged over $5 \cdot 10^5$ realizations for $L = 24, 48, 2 \cdot 10^5$ realizations for $L = 96$ and 10^5 realization for $L \geq 192$. The dashed line in Fig. 2(a) is the analytical prediction. The data converge to this prediction for sufficiently long times, with some deviations close to the saturation level (obviously the MSD cannot grow beyond the squared half total length of the strands). At short times there is a visible deviation from the analytical prediction.

In order to test the validity of Eq. (9) we plot in Fig. 2(b) the quantity $\langle \Delta n^2(t) \rangle t^{-0.92}$ vs. $t^{-(1-\nu)/(\nu z)} = t^{-0.19}$. The MSD plotted in these rescaled unit is expected to show a linear behavior, which is indeed observed in Fig. 2(b). Also it is important to note that the theory predicts a positive coefficient $C > 0$ in Eq. (9), as discussed in Appendix, and this is indeed consistent with the numerics. Moreover, a fit of the correction gives $\langle n(t)^2 \rangle / t^{0.92} = 0.068(1 + C t^{-0.19})$ where the prefactor $C = 1.294$ is in good agreement with the theoretical prediction 1.726 given by Eq.(A.18). Hence we can conclude that the numerical data are in excellent agreement with the tension propagation theory predictions.

Additional support to the theory is obtained from the analysis of the average time τ to fully zip or unzip. This time is expected to be an increasing function of the strands length L . From Eq.(9) one obtains the asymptotic scaling $\tau \sim L^{\nu z}$. This result can be extended to the next order correction from the analysis of Eq. (9)

$$\tau \sim L^{\nu z} \left(1 - DL^{-(1-\nu)} + \dots \right) \quad (10)$$

with $D > 0$. To confirm it, we first present a log-log plot of τ vs. L in Fig. 3(a), which shows some deviations from the asymptotic behavior $\tau \sim L^{\nu z}$. We then show a plot of $\tau L^{-\nu z}$ vs. $L^{-(1-\nu)}$ in Fig. 3(b). The rescaled data follow a straight line with a negative slope in very good agreement with the prediction of Eq. (10).

V. CONCLUSION

The anomalous dynamics in polymers originates from the tension propagation along the chain: a perturbation on a given position propagates along the polymer backbone creating a viscoelastic memory effect for the motion of individual monomers. A theoretical framework of tension propagation has been developed in the past years for the analysis of polymer translocation [19–23] and the motion of a tagged monomer in polymer [14, 15, 22, 24, 25]. In the translocation dynamics it is a monomer exchange across the pore that generates a long range decay of the memory kernel, while in the tagged monomer motion the same effect is due to the spatial displacement by pulling.

The (un)zipping dynamics analyzed in this paper can be understood as a hybrid of the above two processes. It is the monomer exchange Δn (cf. Fig. 1) between zipped and unzipped sections which creates a long range temporal memory leading to a power-law decaying memory kernel as in Eq. (8). Inspecting the elementary process, we see that the first term in the RHS of Eq. (7) reflects the process entailing the spatial displacement $\vec{r}(n_0, 0) \rightarrow \vec{r}(n_0 + \Delta n, 0)$, while the second term concerns the change in Δn without spatial displacement. The latter is reminiscent to the translocation process entailing the monomer exchange across the pore, while the spatial position of the RC is fixed at the pore site.

The present formalism enabled us to extract the the anomalous diffusion characteristics of the RC including the subleading behavior

$$\langle \Delta n^2(t) \rangle \sim t^\alpha (1 + Ct^{-\alpha_1} + \dots) \quad (11)$$

with analytical expressions for α and α_1 which are found to match very well the numerical simulation data. Since the dominant source of the tension generation comes from the spatial displacement of the RC, a process equivalent to pulling operation (the first term in the RHS of Eq. (7)), the asymptotic anomalous diffusion exponent $\alpha = 2/(\nu z)$ is controlled by that of the tagged monomer diffusion, see Eq. (8), while the subleading exponent $\alpha - \alpha_1 = (1 + \nu)/(\nu z)$ coincides with that expected for the unbiased polymer translocation (see Eq. (9) in Ref. [26]). Note, however, that the translocation problem is complex because of a series of factors (post-propagation behavior, interaction with the pore), and simulations, at least in the unbiased case, are still controversial [26–29].

From broader perspective, we repeat once more the caution on the RC based coarse grained description. The validity of the assumption leading to the Markovian dynamics is generally dependent on the time scale

at hand (say, observation), but as we have shown here, there would exist for the dynamics of long polymers a broad time window, in which collective dynamics among degrees of freedom with varying time scale manifests. The resulting non-Markovian dynamics should be of pronounced importance in the context of biopolymer functions. Although more work is necessary to fully unveil the consequences, our analytical argument for the MSD is regarded a first step toward such an ambitious goal.

Finally, we note that the process is biased away from the critical point. At low temperatures the hairpin folding process exhibits out-of-equilibrium characteristics [30] reminiscent of polymer translocation driven by external bias [19, 21, 23, 26, 31, 32]. Here again, a key physics lies in the tension propagation, the dynamics of which bears distinctive features not seen in the unbiased regime.

ACKNOWLEDGMENTS

This work is supported by KAKENHI (No. 16H00804, Fluctuation and Structure) from MEXT, Japan, and JST, PREST. This work is also part of the program (AAP 2013-2-005, 2015-2-055, 2016-1-024).

Appendix: The correction to scaling behavior

We give here the full derivation of the calculation of the MSD including the subleading corrections. The calculation consists of two steps. Firstly we determine the mobility kernel $\mu(t)$ and from it, using the FDT, we obtain the MSD.

1. Mobility Kernel

Taking the Laplace transforms of Eqs. (1) and (3) one obtains the following relation:

$$\hat{\mu}(s) = \frac{1}{\hat{\gamma}(s)} \quad (\text{A.1})$$

(generalizing the relation between mobility and friction). In the previous equation $\hat{\gamma}(s)$ and $\hat{\mu}(s)$ are the Laplace transforms of $\gamma(t)$ and $\mu(t)$, respectively. In what follows we calculate the Laplace transform of the memory kernel $\hat{\gamma}(s)$ and then obtain $\hat{\mu}(s)$ from Eq. (A.1). Finally we use the inverse Laplace transform to obtain $\mu(t)$. This can be readily done for a pure power law function $\gamma(t) = t^{-\alpha}$: its Laplace transform is $\hat{\gamma}(s) = \Gamma(1 - \alpha)s^{\alpha-1}$, where $\Gamma(z)$ is the Euler gamma function. Therefore, neglecting the prefactor, $\hat{\mu}(s) \sim s^{1-\alpha}$ which leads to $\mu(t) \sim t^{\alpha-2}$. This is the result mentioned at the end of Section II.

Let us start now from the memory kernel which includes a subleading correction at long times:

$$\gamma(t) \simeq \frac{k_B T}{a^2} t^{-2/z} \left[1 - \nu t^{-\frac{\nu+1}{\nu z} + \frac{2}{z}} \right] \quad (\text{A.2})$$

where the time is made dimensionless with the unit τ_0 . Its Laplace transform is:

$$\hat{\gamma}(s) = \frac{k_B T}{a^2} \left[\Gamma\left(1 - \frac{2}{z}\right) s^{2/z-1} - \nu \Gamma\left(1 - \frac{\nu+1}{\nu z}\right) s^{\frac{\nu+1}{\nu z}-1} \right] = \frac{k_B T}{A a^2} s^{2/z-1} \left[1 - B s^{\frac{\nu+1}{\nu z}-2/z} \right] \quad (\text{A.3})$$

where we have introduced

$$B \equiv \nu \frac{\Gamma(1 - \frac{\nu+1}{\nu z})}{\Gamma(1 - 2/z)} > 0 \quad (\text{A.4})$$

and

$$A^{-1} \equiv \Gamma(1 - 2/z) > 0 \quad (\text{A.5})$$

From (A.1) and (A.3) we get

$$\hat{\mu}(s) = \frac{a^2}{k_B T} A s^{1-2/z} \left[1 - B s^{\frac{\nu+1}{\nu z}-2/z} \right]^{-1} \quad (\text{A.6})$$

The inverse Laplace transform can be calculated using the Mittag-Leffler function [33]. However, in order to avoid possible convergence issues we will only calculate $\mu(t)$ in the long time limit, which corresponds to the small s approximation of (A.6). In that limit we get

$$\hat{\mu}(s) = \frac{a^2}{k_B T} A \left[s^{-\kappa} + B s^{-\epsilon-\kappa} + \dots \right] \quad (\text{A.7})$$

where $\epsilon = 2/z - (\nu+1)/(\nu z) < 0$ and $\kappa = 2/z - 1 < 0$. The inverse Laplace transform of (A.7) is given by

$$\mu(t) = \frac{a^2}{k_B T} A \left[\frac{t^{\kappa-1}}{\Gamma(\kappa)} + B \frac{t^{\epsilon+\kappa-1}}{\Gamma(\epsilon+\kappa)} \right] \quad (\text{A.8})$$

2. Mean squared displacement of the reaction coordinate

In absence of forces Eq. (3) becomes

$$\vec{v}(t) = \vec{\eta}(t) \quad (\text{A.9})$$

where

$$\langle \eta_i(t) \eta_j(s) \rangle = k_B T \mu(|t-s|) \delta_{ij} \quad (\text{A.10})$$

From (A.9) we get for the mean squared displacement (MSD) $\Delta \vec{x}^2(t) = \langle (\vec{x}(t) - \vec{x}(0))^2 \rangle$

$$\Delta \vec{x}^2(t) = 3 \int_0^t \int_0^t \langle \eta(t_1) \eta(t_2) \rangle dt_1 dt_2 \quad (\text{A.11})$$

Therefore using (A.10) and (A.8) we get

$$\Delta \vec{x}^2(t) = 3a^2 A \int_0^t \int_0^t \left[\frac{|t_1 - t_2|^{\kappa-1}}{\Gamma(\kappa)} + B \frac{|t_1 - t_2|^{\epsilon+\kappa-1}}{\Gamma(\epsilon+\kappa)} \right] dt_1 dt_2 \quad (\text{A.12})$$

Integrals of the type

$$I = \int_0^t \int_0^t |t_1 - t_2|^\sigma dt_1 dt_2 \quad (\text{A.13})$$

are easily performed. First, from the symmetry between t_1 and t_2 we get

$$I = 2 \int_0^t \left(\int_0^{t_1} (t_1 - t_2)^\sigma dt_2 \right) dt_1 \quad (\text{A.14})$$

and then switching to $y = t_2/t_1$

$$I = 2 \int_0^t t_1^{\sigma+1} dt_1 \int_0^1 (1-y)^\sigma dy = \frac{2t^{2+\sigma}}{(2+\sigma)(1+\sigma)} \quad (\text{A.15})$$

provided $\sigma > -1$. Otherwise we get a divergence at the origin. However, physically we can always introduce a small cutoff and take the initial time to be some small time t_ϵ . This will add a constant to the result (A.15).

Inserting (A.15) into (A.12) we get

$$\Delta \vec{x}^2(t) = 6a^2 A \left[\frac{t^{\kappa+1}}{\kappa(\kappa+1)\Gamma(\kappa)} + B \frac{t^{1+\kappa+\epsilon}}{\Gamma(\epsilon+\kappa)(\kappa+1+\epsilon)(\kappa+\epsilon)} + \dots \right]$$

Using the relation $z\Gamma(z) = \Gamma(z+1)$,

$$\Delta \vec{x}^2(t) = 6a^2 A \left[\frac{t^{1+\kappa}}{\Gamma(\kappa+2)} + B \frac{t^{\epsilon+\kappa+1}}{\Gamma(\kappa+\epsilon+2)} + \dots \right] \quad (\text{A.16})$$

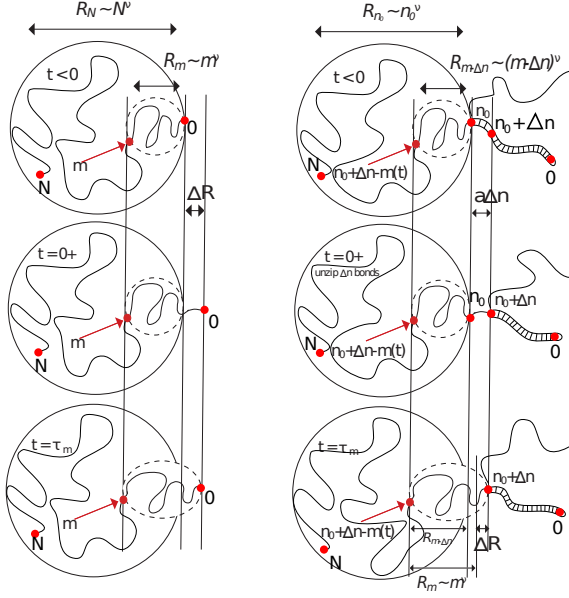


FIG. 1. (a) Illustration of the propagation of the tension in a polymer pulled at one end. (i) Initial state ($t < 0$): the polymer is at equilibrium ($R_N \sim N^\nu$). We discern the section of the polymer reached by the tension at time τ_m , containing $m(\tau_m)$ monomers (equilibrium size $R_m \sim m(\tau_m)^\nu$). (ii) Application of the pulling force \vec{f} at the monomer 0 ($t = 0^+$). The polymer is stretched at one end. (iii) Propagation of the tension until monomer $m(\tau_m)$ ($t = \tau_m$): the section between monomers 0 and $m(\tau_m)$ is now sharing the stretching, its size becomes $R_m + \Delta R$. This difference in size leads to an elastic-like force driving the tension further along the polymer. (b) Illustration of a zipping polymer and the peeling operation (performed over Δn monomers) applied to measure the stress relaxation associated to the tension propagation. (i) Initial state ($t < 0$): the single strands are at equilibrium and contains each n_0 monomers (equilibrium size $R_{n_0} \sim n_0^\nu$). Anticipating the tension front at $t = \tau_m$, we discern the section with $m(\tau_m)$ monomers, whose equilibrium size is $R_{m-\Delta n} \sim (m - \Delta n)^\nu$. (ii) Application of the perturbation at $t = 0^+$: the peeling operation is applied on Δn monomers, which are thus added to the single stranded polymers. This difference makes the system more complex than the pulled polymer. The peeling create a local tension between monomers n_0 and $n_0 + \Delta n$, which will propagate. (iii) Propagation of the tension at time $t = \tau_m$: the tension front reaches the monomer $n_0 + \Delta n - m(\tau_m)$. The tension is now shared by $m(\tau_m)$ monomers starting from $n_0 + \Delta n$. The difference between the expected size at equilibrium $R_m \sim m^\nu$ and the actual size resulting from the tension $R_{m-\Delta n} + a\Delta n \sim (m - \Delta n)^\nu + a\Delta n$ gives rise to an elastic force that drives the tension further along the polymer.

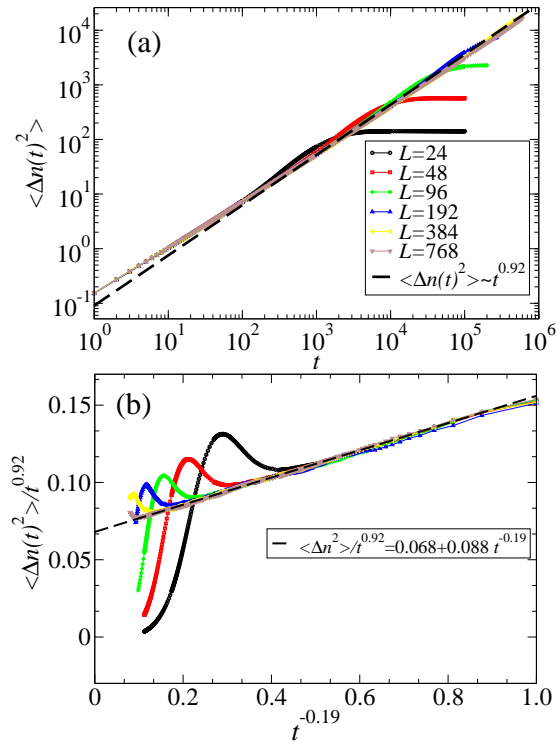


FIG. 2. (a) The mean-square displacement $\langle \Delta n(t)^2 \rangle$ of the reaction coordinate (fork location along the chain) is plotted versus time for different sizes. The symbols are obtained for simulations with different sizes (from [13]). The dashed line is the theoretical prediction with an exponent 0.92. (b) Correction to scaling $\langle \Delta n(t)^2 \rangle / t^{0.92}$ plotted versus $t^{-0.19}$. According to Eq.(9), the resulting curve should fit linearly. Remarkably, even the numerical value of the slope of the corrections are in good agreement with theory. For both the leading and first order correction to scaling, the numerics are in very good agreements with numerics.

We next go from motion in physical space to motion in monomer space through the relation $\Delta \vec{x}^2(t) \sim [\Delta n^2(t)]^\nu$. Inserting in (A.16) gives our final result from which one can read off the leading correction to the

asymptotic scaling

$$\Delta n^2(t) \sim t^{(1+\kappa)/\nu} \left[1 + \frac{B\Gamma(\kappa+2)}{\nu\Gamma(\kappa+\epsilon+2)} t^\epsilon + \dots \right] \quad (\text{A.17})$$

Inserting $\nu = .588$ then gives

$$\langle \Delta n^2(t) \rangle \sim t^{.92} [1 + C t^{-0.19} + \dots] \quad (\text{A.18})$$

where the prefactor C in front of the correction is positive, whose value is calculated as $C \approx 1.695B \approx 1.726$ for the present case ($z = 1 + 2\nu$ with $\nu = 0.588$).

-
- [1] N. van Kampen, *Stochastic processes in Physics and Chemistry* (Elsevier, 1995)
 - [2] B. B. Mandelbrot and J. W. V. Ness, SIAM Review **10**, 422 (1968)
 - [3] J.-P. Bouchaud and A. Georges, Physics Reports **195**,

- 127 (1990)
- [4] F. Amblard, A. C. Maggs, B. Yurke, A. N. Pargellis, and S. Leibler, Phys. Rev. Lett. **77**, 4470 (1996)
- [5] J. Krug, H. Kallabis, S. Majumdar, S. Cornell, A. Bray, and C. Sire, Phys. Rev. E **56**, 2702 (1997)

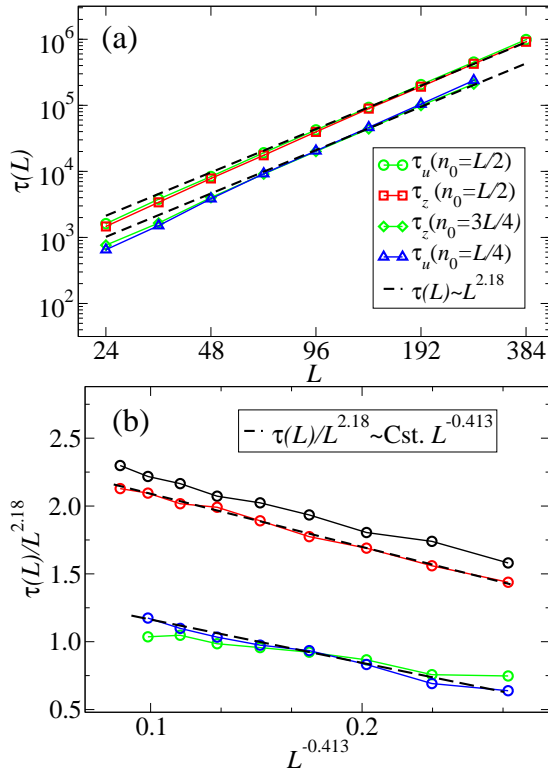


FIG. 3. (a) The (un)zipping time is plotted versus the polymer length for different initial conditions ($n_0 = 1/4, 1/2$ and $3/4$). Symbols are results from simulations, and Eq.(10). The analytical estimate of the exponent 2.18 is in good agreement with the numerics for large sizes. (b) $\tau(L)/L^{2.18}$ is plotted versus the first order correction to scaling $t^{-0.413}$. The resulting curve is expected to be a straight line with a negative slope. Both leading term and first order correction are in good agreement with the numerics.

- [6] R. Metzler and J. Klafter, Phys. Rep. **339**, 1 (2000)
- [7] D. Panja, G. T. Barkema, and A. B. Kolomeisky, J. Phys.: Condens. Matter **21**, 242101 (2009)
- [8] A. Amitai, Y. Kantor, and M. Kardar, Phys. Rev. E **81**,

- 011107 (2010)
- [9] L. Lizana, T. Ambjörnsson, A. Taloni, E. Barkai, and M. A. Lomholt, Phys. Rev. E **81**, 051118 (2010)
- [10] T. Akimoto, E. Yamamoto, K. Yasuoka, Y. Hirano, and M. Yasui, Phys. Rev. Lett. **107**, 178103 (2011)
- [11] R. Metzler, J.-H. Jeon, A. G. Cherstvy, and E. Barkai, Phys. Chem. Chem. Phys. **16**, 24128 (2014)
- [12] M. Manghi and N. Destainville, Phys. Rep. **631**, 1 (2016)
- [13] J.-C. Walter, A. Ferrantini, E. Carlon, and C. Vanderzande, Phys. Rev. E **85**, 031120 (2012)
- [14] T. Sakaue, T. Saito, and H. Wada, Phys. Rev. E **86**, 011804 (2012)
- [15] T. Saito and T. Sakaue, Phys. Rev. E **92**, 012601 (2015)
- [16] A. Ferrantini, M. Baiesi, and E. Carlon, J. Stat. Mech.: Theory and Exp. **2010**, P03017 (2010)
- [17] A. Ferrantini and E. Carlon, J. Stat. Mech.: Theory and Exp. **2011**, P02020 (2011)
- [18] T. Ishinabe, Phys. Rev. B **39**, 9486 (1989)
- [19] T. Sakaue, Phys. Rev. E **76**, 021803 (2007)
- [20] D. Panja, G. T. Barkema, and R. C. Ball, J. Phys.: Condens. Matter **19**, 432202 (2007)
- [21] T. Sakaue, Phys. Rev. E **81**, 041808 (2010)
- [22] D. Panja, J. Stat. Mech.: Theory and Exp. **2010**, P06011 (2010)
- [23] T. Ikonen, T. Ala-Nissila, A. Bhattacharya, and W. Sung, J. Chem. Phys. **137**, 085101 (2012)
- [24] P. Rowghanian and A. Y. Grosberg, Phys. Rev. E **86**, 011803 (2012)
- [25] H. Vandebroek and C. Vanderzande, J. Chem. Phys. **141**, 114910 (2014)
- [26] T. Sakaue, Polymers **8**, 424 (2016)
- [27] J. Chuang, Y. Kantor, and M. Kardar, Phys. Rev. E **65**, 011802 (2001)
- [28] H. W. de Haan and G. W. Slater, J. Chem. Phys. **136**, 154903 (2012)
- [29] V. V. Palyulin, T. Ala-Nissila, and R. Metzler, Soft matter **10**, 9016 (2014)
- [30] R. Frederickx, T. In't Veld, and E. Carlon, Phys. Rev. Lett. **112**, 198102 (2014)
- [31] V. V. Lehtola, R. P. Linna, and K. Kaski, EPL (Europhysics Letters) **85**, 58006 (2009)
- [32] A. Bhattacharya and K. Binder, Phys. Rev. E **81**, 041804 (2010)
- [33] H. J. Haubold, A. M. Mathai, and R. K. Saxena, J. Appl. Math. **2011**, 298628 (2011)